Electronic Supplementary Material (ESI) for ChemComm.

Electronic Supporting Information

Single-component frameworks for heterogeneous catalytic hydrolysis of organophosphatesorous compounds in pure water

Sergio J. Garibay,[a] Omar K. Farha*[b] and Jared B. DeCoste*[a]

[a]*Combat Capabilities Development Command Chemical Biological Center, 5183 Blackhawk Road, Aberdeen Proving Ground, Maryland 21010, USA*
[b]*Department of Chemistry, Northwestern University, 2145 Sheridan Road, Evanston, Illinois 60208, USA*

*Corresponding authors: jared.b.decoste2.civ@mail.mil , o-farha@northwestern.edu

Experimental Procedures

All reagents were purchased from commercial sources and used without further purification. H_4TBAPy was synthesized following published procedures.[1-3] NU-901, NU-901-act, NU-901-SALI-nico, and NU-901-SALI-BA-$N(CH_3)_2$ were synthesized following a published procedure.[4]

^{1}H-NMR spectra were recorded on Varian FT-NMR spectrometer (300 MHz) and data were analysed with Mestre Nova software. Samples (~10 mg) were digested using ~60 μL of D_2SO_4 and 600 μLof DMSO-d_6.

^{31}P-NMR spectra were recorded on Varian FT-NMR spectrometer (400 MHz) and data were analysed with Mestre Nova software.

Powder X-ray diffraction (PXRD) data were measured at room temperature on a STOE-STADIMP powder diffractometer equipped with an asymmetric curved Germanium monochromator (CuKα1 radiation, λ = 1.54056 Å) and one-dimensional silicon strip detector (MYTHEN2 1K from DECTRIS). The line focused Cu X-ray tube was operated at 40 kV and 40 mA. The activated powder was sandwiched between two Kapton foils and measured in transmission geometry in a rotating holder. Intensity data from 2 to 30 degrees two theta were collected over a period of 15 min. The instrument was calibrated against a NIST Silicon standard (640d) prior to the measurement. PXRD data were also measured on a Rigaku Miniflex 600 diffractometer at 30kV, 15mA (CuKα1 radiation, λ = 1.54056 Å) with a scan speed of 5°/min and a step size of 0.05 in 2θ at room temperature

Nitrogen isotherm measurements were carried out on a Micromeritics ASAP 2420 instrument at 77 K. Samples were activated at specified temperatures under vacuum on a Micromeritics Smart VacPrep instrument until an outgas rate below 0.05 mmHg/min was achieved.

HCl-activation of NU-901: The as synthesized NU-901 was suspended in 12 mL DMF and 0.5 mL of 8 M aqueous HCl was added to a 8-dram vial and heated in an oven at 100^{0}C for 18 h. After cooling to room temperature, the powder was isolated by centrifugation and washed with DMF three times (10 mL each) and acetone three times (10 mL each). NU-901-act was collected by centrifugation and dried in a vacuum oven at 80 ^{0}C for 1 h, and then activated at 120 ^{0}C for 18 h using Micromeritics Smart VacPrep instrument as described above.

Synthesis of NU-901-SALI-[nico]$_2$: NU-901-act (33 mg, 0.0162 mmol) and nicotinic acid (58 mg, 0.26 mmol) were mixed in 8 mL of DMF in an 8-dram vial and ultrasonically dissolved. The clear solution was incubated in an oven at 60 ^{0}C for 18 h. After cooling down to room temperature, material was isolated by centrifuge (5 min, 7500 rpm) and solvent exchanged with fresh DMF three times (10 mL each) followed by methanol three times (10 mL). NU-901-SALI-[nico]$_2$ was collected by centrifugation and dried in a vacuum oven at 80 ^{0}C for 1 h, and then activated at 120 ^{0}C for 18 h using Micromeritics Smart VacPrep instrument as described above.

Synthesis of NU-901-SALI-[BA-morph]$_{3.5}$: NU-901-act (33 mg, 0.016 mmol) and 4-(morpholinomethyl)benzoic acid (58 mg, 0.26 mmol) were mixed in 8 mL of DMF in an 8-dram vial and ultrasonically dissolved. The clear solution was incubated in an oven at 60 ^{0}C for 18 h. After cooling down to room temperature, material was isolated by centrifuge (5 min, 7500 rpm) and solvent exchanged with fresh DMF three times (10 mL each) followed by methanol three times (10 mL). NU-901-SALI-[morph]$_{3.5}$ was collected by centrifugation and dried in a vacuum oven at 80 ^{0}C for 1 h, and then activated at 120 ^{0}C for 18 h using Micromeritics Smart VacPrep instrument as described above.

Synthesis of NU-901-SALI-[BA-morph]$_2$: NU-901-act (28 mg, 0.013 mmol) and 4-(morpholinomethyl)benzoic acid (6 mg, 0.028 mmol) were mixed in 8 mL of DMF in an 8-dram vial and ultrasonically dissolved. The clear solution was incubated in an oven at 65 ^{0}C for 18 h. After cooling down to room temperature, material was isolated by centrifuge (5 min, 7500 rpm) and solvent exchanged with fresh DMF three times (10 mL each) followed by methanol three times (10 mL). NU-901-SALI-[BA-morph]$_2$ was collected by centrifugation and dried in a vacuum oven at 80 ^{0}C for 1 h, and then activated at 120 ^{0}C for 18 h using Micromeritics Smart VacPrep instrument as described above.

Synthesis of NU-901-SALI-[BA-CH$_2$NH$_2$]$_2$: NU-901-act (45 mg, 0.03 mmol) and 4-(aminomethyl)benzoic acid (73 mg, 0.048 mmol) were mixed in 16 mL of H_2O in an 8-dram vial and ultrasonically dissolved. The clear solution was incubated in an oven at 60 ^{0}C for 18 h. After cooling down to room temperature, material was isolated by centrifuge (5 min, 7500 rpm) and solvent exchanged with fresh H_2O three times (10 mL each) followed by methanol three times (10 mL). NU-901-SALI-[BA-CH$_2$NH$_2$]$_2$ was collected by centrifugation and dried in a vacuum oven at 80 ^{0}C for 1 h, and then activated at 120 ^{0}C for 18 h using Micromeritics Smart VacPrep instrument as described above.

MOF-808 synthesis and HCl activation: $ZrCl_4$ (117 mg, 0.5 mmol), BTC (35 mg, 0.168 mmol) and propanoic acid (3.7 mL, 49 mmol) were mixed in 10 mL of DMF in an 8-dram vial and ultrasonically dissolved. The clear solution was incubated in an oven at 120 ^{0}C for 24 h. After cooling down to room temperature, the white polycrystalline material was isolated by centrifuge (5 min, 7500 rpm) and solvent exchanged with fresh DMF three times (10 mL each) followed by methanol three times (10 mL). MOF-808-P was collected by centrifugation and dried in a vacuum oven at 80 ^{0}C for 1 h.

The as synthesized MOF-808-P was suspended in 12 mL DMF and 0.5 mL of 4 M aqueous HCl was added to an 8-dram vial and heated in an oven at 100^{0}C for 18 h. After cooling to room temperature, the powder was isolated by centrifugation and washed with DMF three times (10 mL each) and acetone three times (10 mL each). MOF-808-act was collected by centrifugation and dried in a vacuum oven at 80 ^{0}C for 1 h, and then activated at 120 ^{0}C for 18 h using Micromeritics Smart VacPrep instrument as described above.

Synthesis of MOF-808-SALI-[BA-morph]$_3$: MOF-808-act (106 mg, 0.07 mmol) and 4-(morpholinomethyl)benzoic acid (309 mg, 0.028 mmol) were mixed in 8 mL of DMF in an 8-dram vial and ultrasonically dissolved. The clear solution was incubated in an oven at 70 ^{0}C for 48 h. After cooling down to room temperature, material was isolated by centrifuge (5 min, 7500 rpm) and solvent exchanged with fresh DMF three times (10 mL each) followed by methanol three times (10 mL). MOF-808-SALI-[BA-morph]$_3$ was collected by centrifugation and dried in a vacuum oven at 80 ^{0}C for 1 h, and then activated at 100 ^{0}C for 18 h using Micromeritics Smart VacPrep instrument as described above.

Synthesis of MOF-808-SALI-[BA-CH$_2$NH$_2$][BA-CH2-NH$_3^+$]: MOF-808-act (112 mg, 0.073 mmol) and 4-(aminomethyl)benzoic acid (220 mg, 1.5 mmol) were mixed in 8 mL of H_2O in an 8-dram vial and ultrasonically dissolved. The clear solution was incubated in an oven at 70 ^{0}C for 48 h. After cooling down to room temperature, material was isolated by centrifuge (5 min, 7500 rpm) and solvent exchanged with fresh H_2O three times (10 mL each) followed by methanol three times (10 mL). MOF-808-SALI-[BA-CH$_2$NH$_2$][BA-CH$_2$-NH$_3^+$] was collected by

centrifugation and dried in a vacuum oven at 80 ^{0}C for 1 h, and then activated at 100 ^{0}C for 18 h using Micromeritics Smart VacPrep instrument as described above.

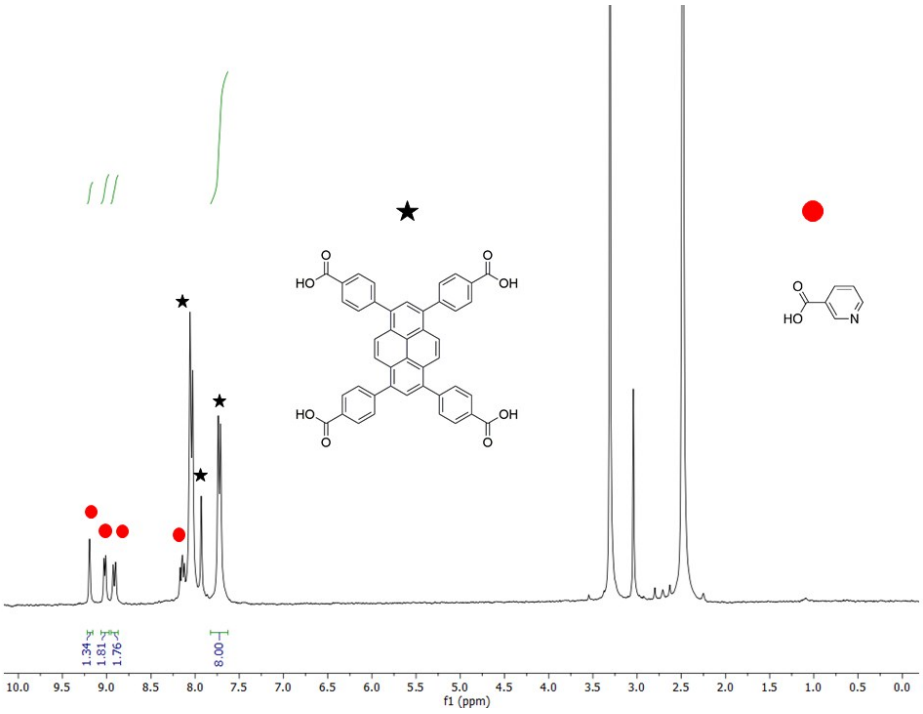

Figure S1. ^{1}H NMR spectrum of digested NU-901-SALI-[nico]$_2$ in d_6-DMSO.

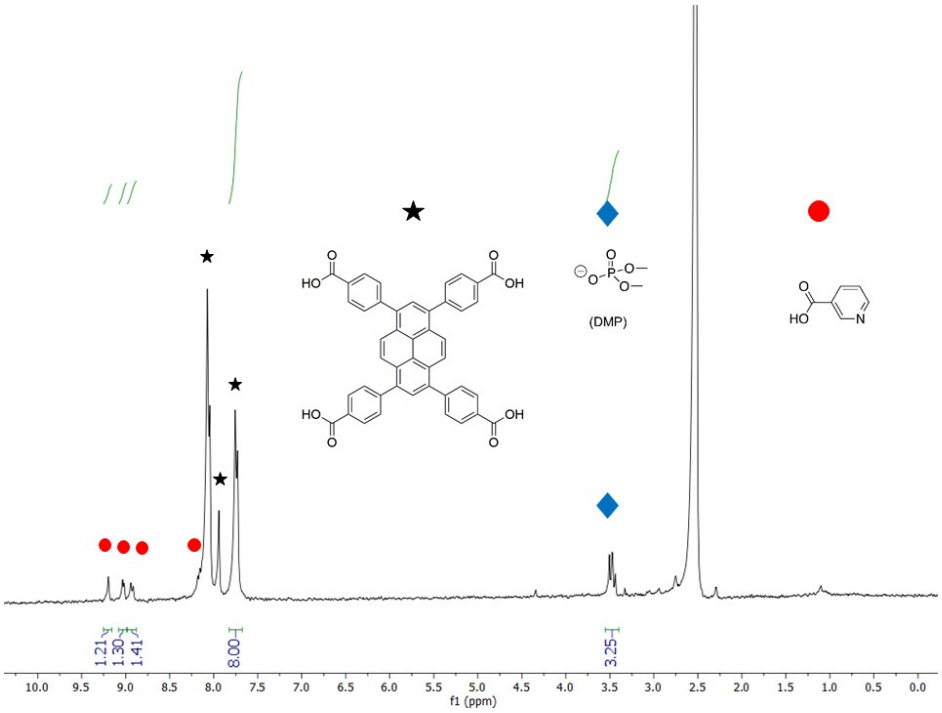

Figure S2. ^{1}H NMR spectrum of digested NU-901-SALI-[nico]$_2$ post reaction in d_6-DMSO.

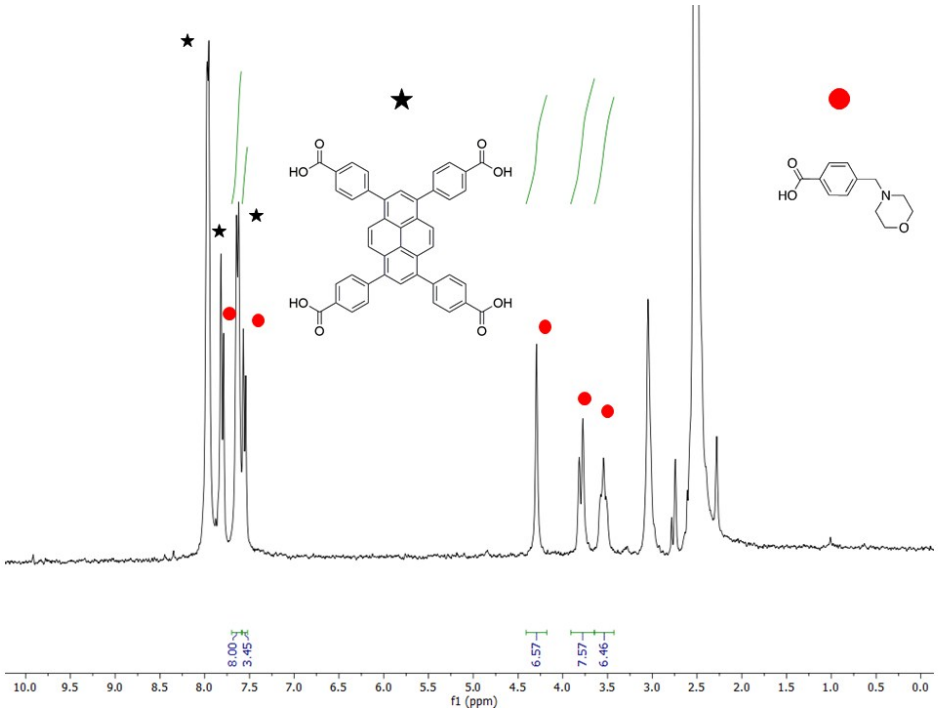

Figure S3. ^{1}H NMR spectrum of digested NU-901-SALI-[BA-morph]$_{3.5}$ in d_6-DMSO.

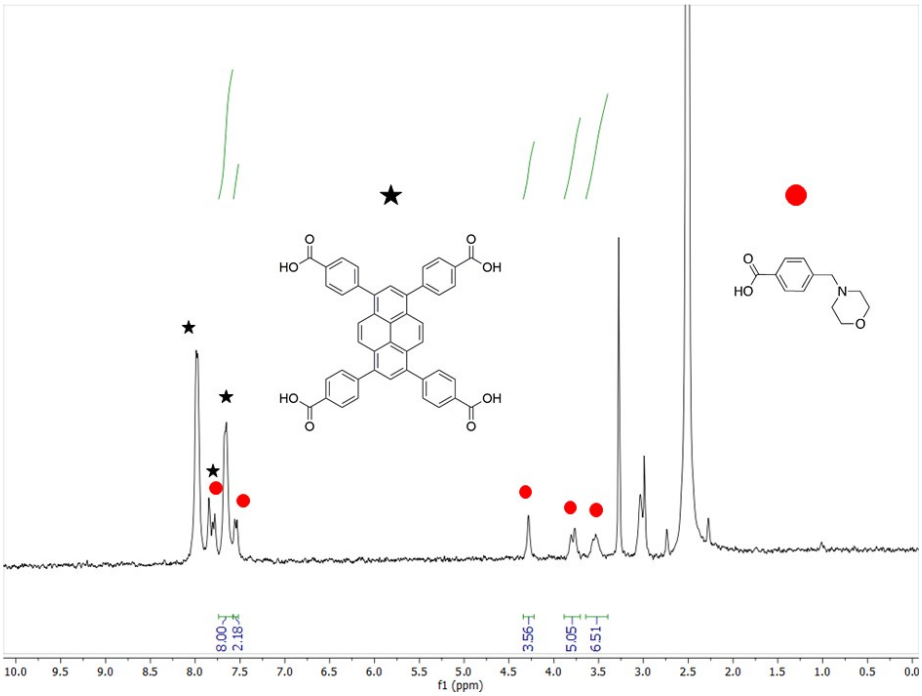

Figure S4. ^{1}H NMR spectrum of digested NU-901-SALI-[BA-morph]$_{2}$ in d_6-DMSO.

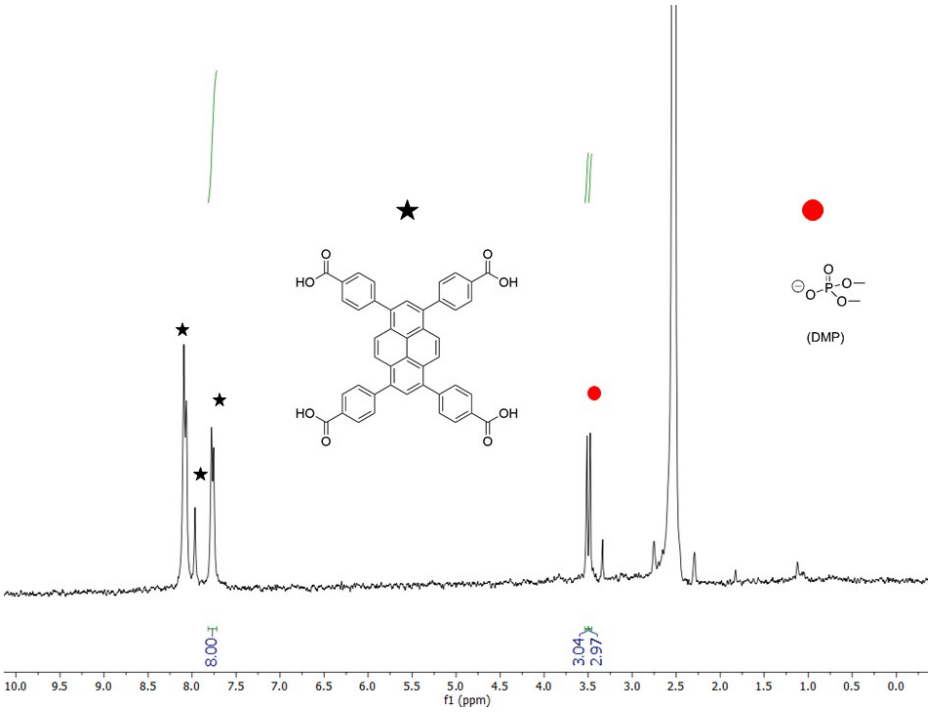

Figure S5. ^{1}H NMR spectrum of digested NU-901-SALI-[BA-morph]$_{3.5}$ post reaction in d_6-DMSO.

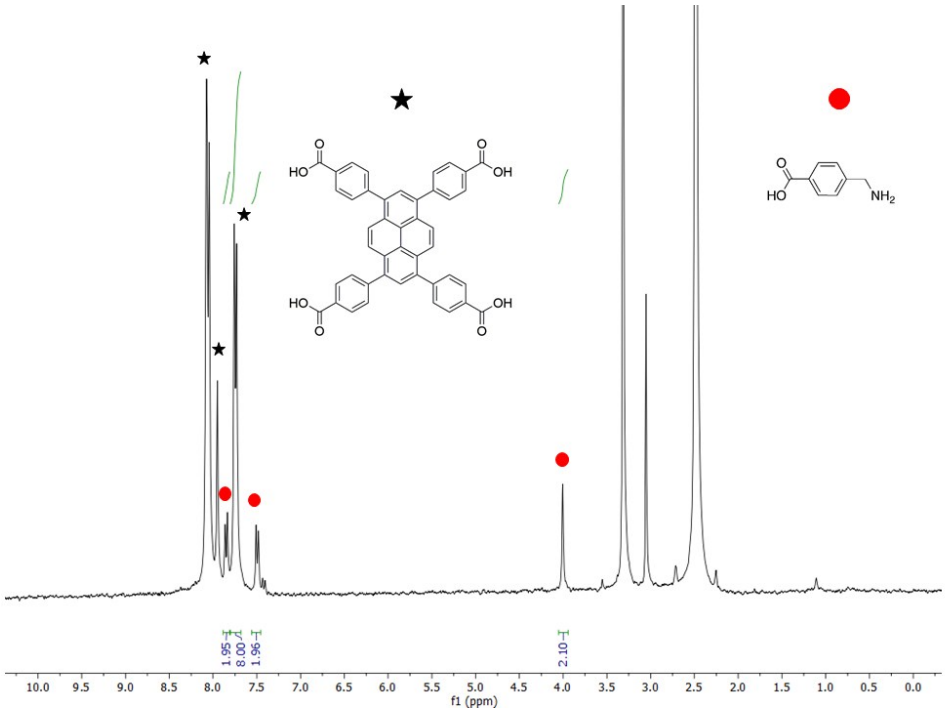

Figure S6. ^{1}H NMR spectrum of digested NU-901-SALI-[BA-CH_2NH_2]$_2$ in d_6-DMSO.

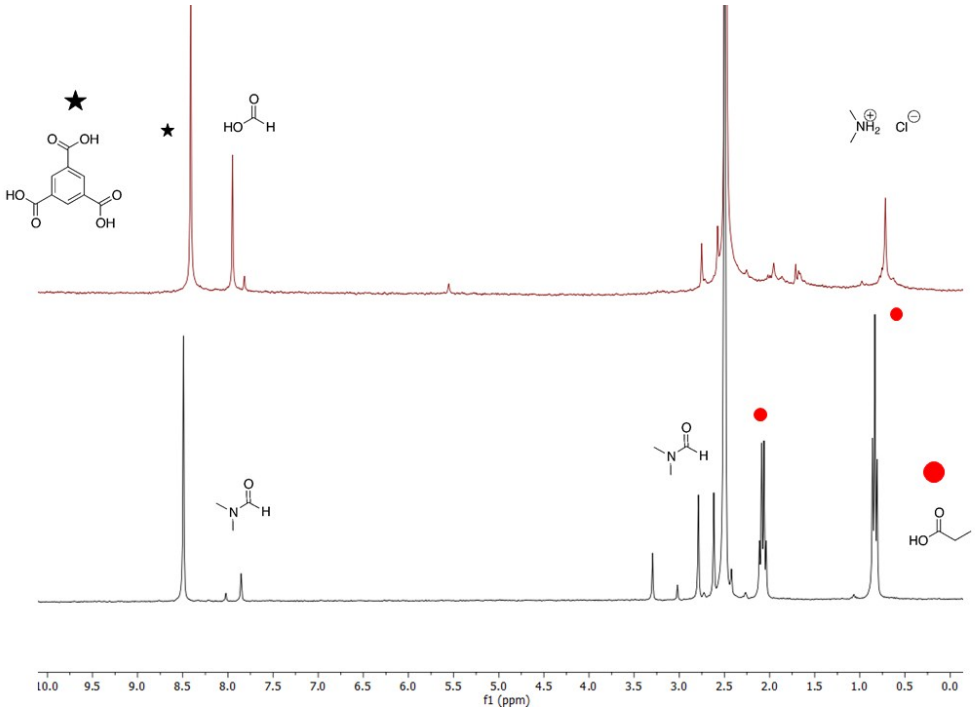

Figure S7. ^{1}H NMR spectrum of digested MOF-808-P (bottom), DMF-HCl activated MOF-808 (middle) and EtOH-HCl activated MOF-808 (top) in d_6-DMSO.

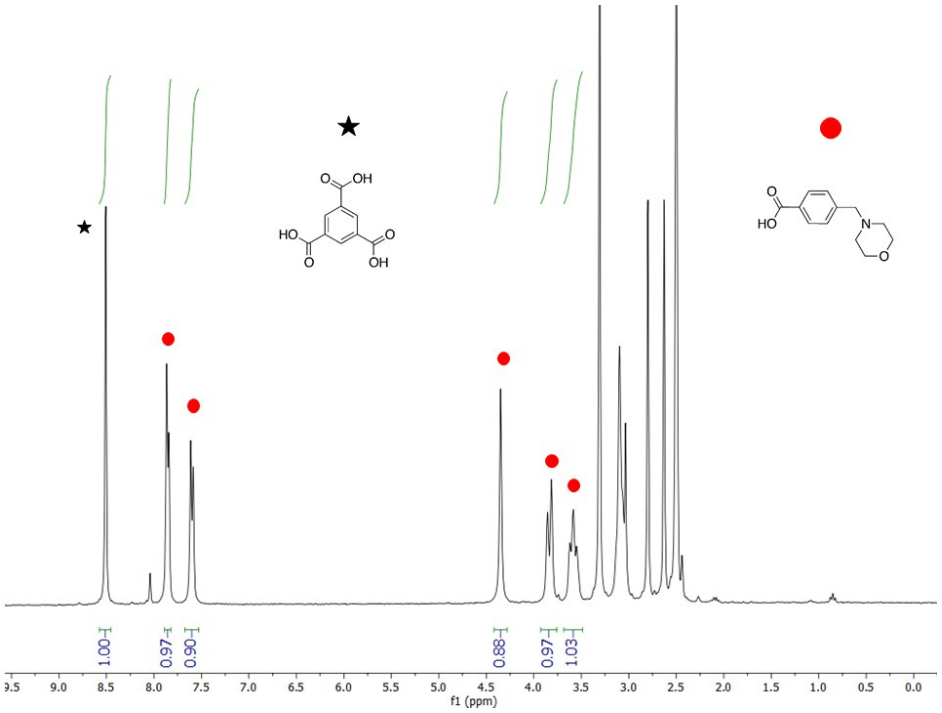

Figure S8. ^{1}H NMR spectrum of digested MOF-808-SALI-[BA-morph]$_3$ in d_6-DMSO.

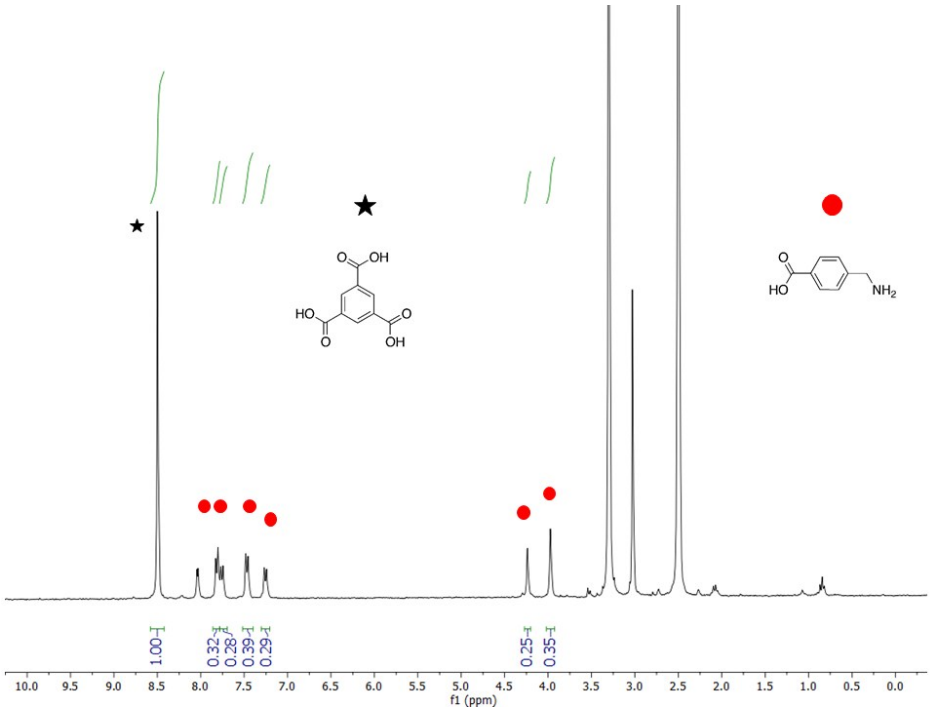

Figure S9. ^{1}H NMR spectrum of digested MOF-808-SALI-[BA-CH_2NH_2][BA-CH_2-NH_3^+] in d_6-DMSO.

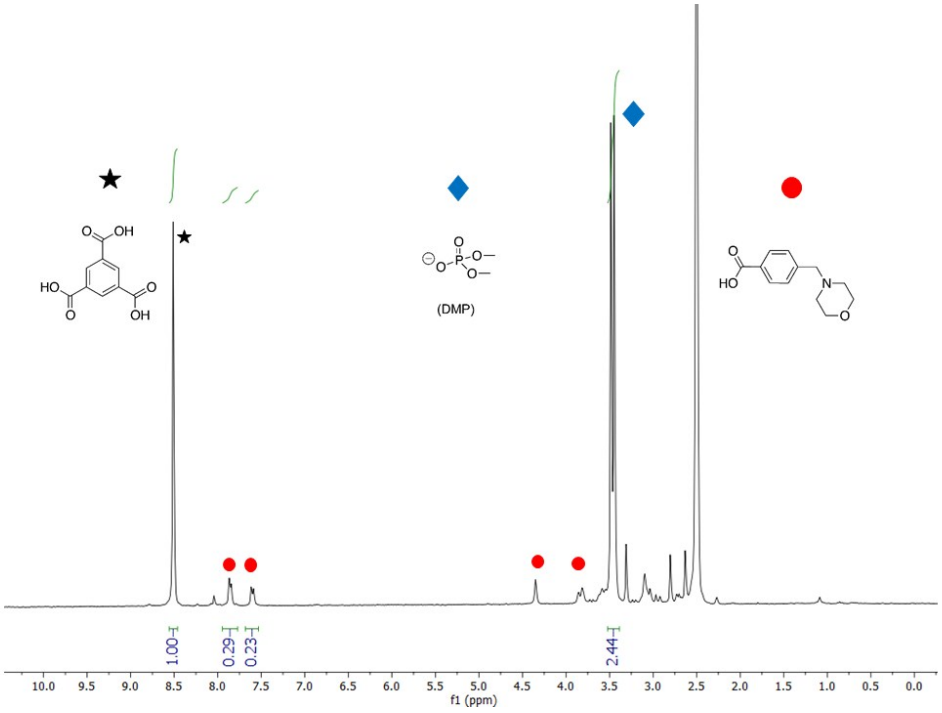

Figure S10. ^{1}H NMR spectrum of digested of MOF-808-SALI-[BA-morph]$_3$ post reaction in d_6-DMSO.

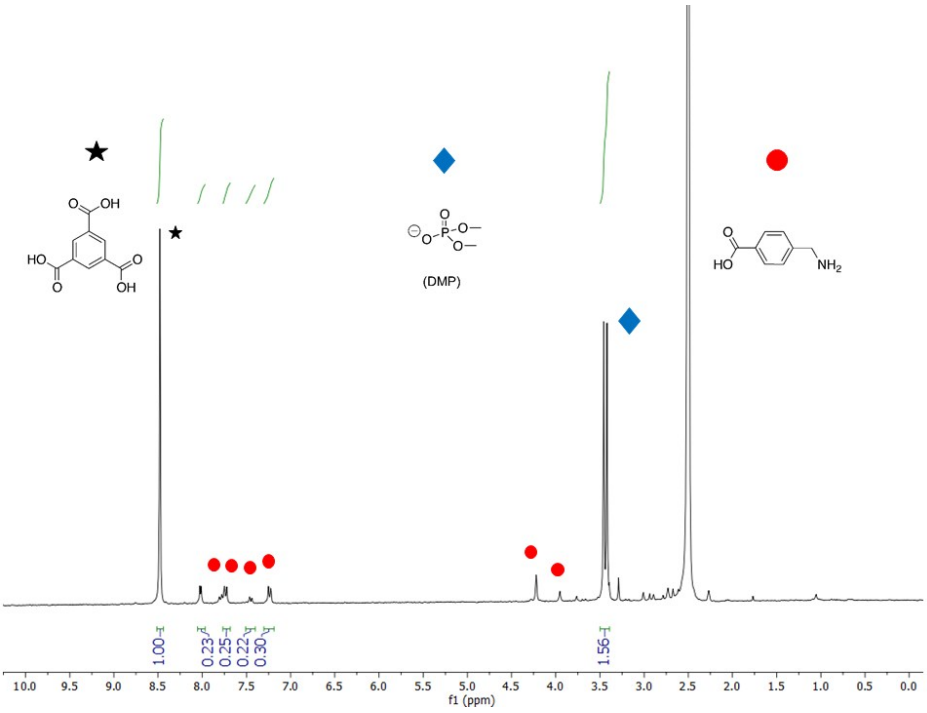

Figure S11. ^{1}H NMR spectrum of digested of MOF-808-SALI-[BA-CH_2NH_2][BA-CH_2-NH_3^+] post reaction in d_6-DMSO.

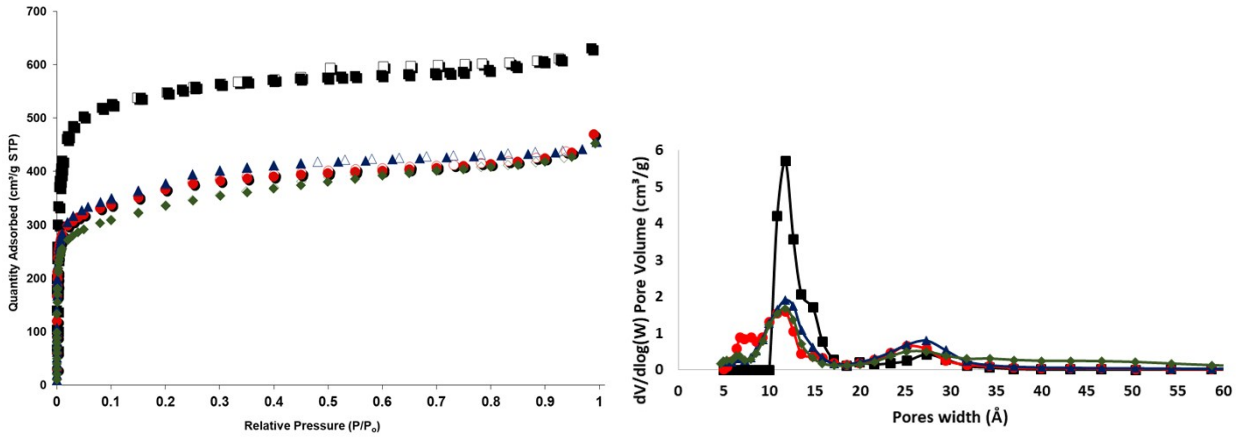

Figure S12. N_2 isotherms of NU-901-act (black squares), NU-901-SALI-[BA-morph]$_{3.5}$ (red circles), and NU-901-SALI-[BA-morph]$_2$ (blue triangles), and NU-901-SALI-[BA-CH_2NH_2]$_2$ (green diamonds). Adsorption = filled, desorption = empty markers.

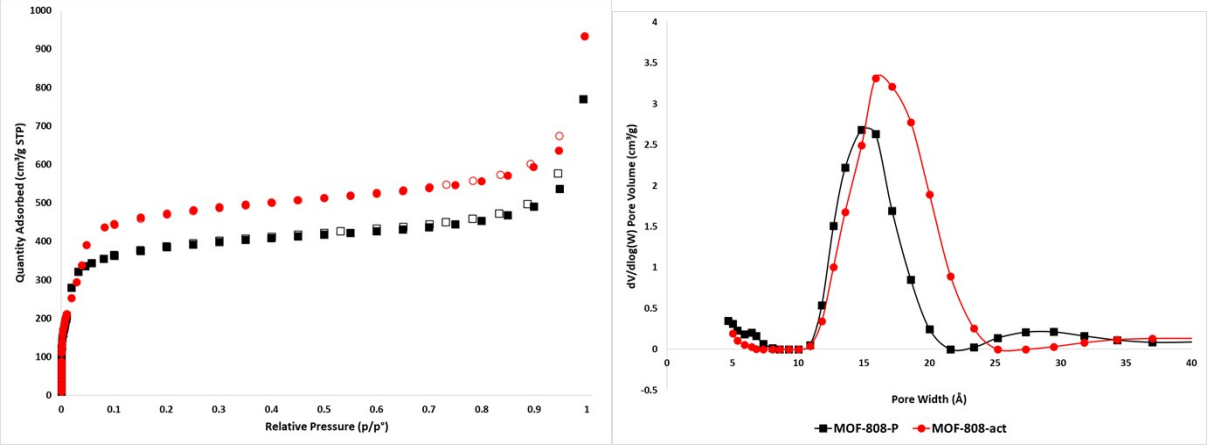

Figure S13. N_2 isotherms (left) and pore size distribution (right) of MOF-808-P (black squares) and MOF-808-act (red circles). Adsorption = filled, desorption = empty markers.

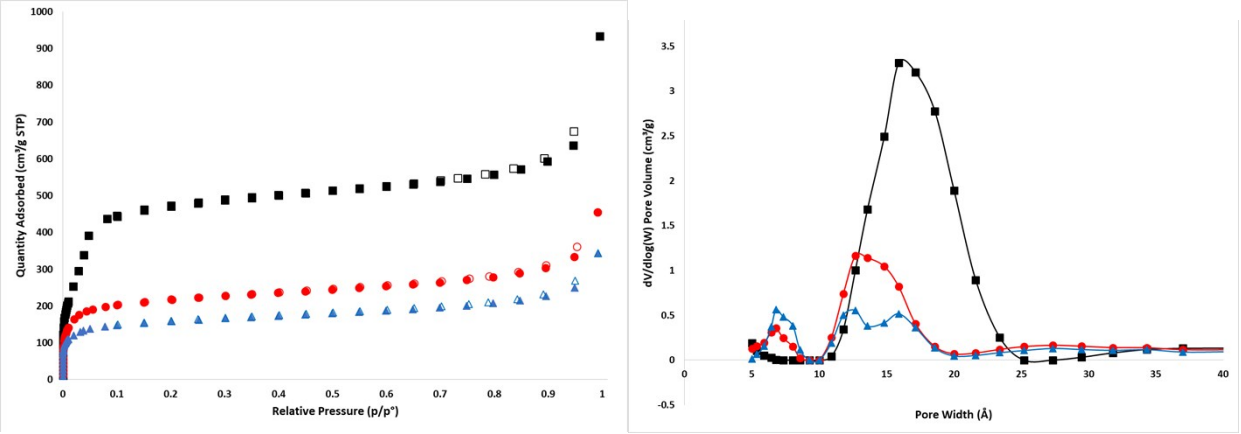

Figure S14. N_2 isotherms (left) and pore size distribution (right) of MOF-808-act (black squares), MOF-808-SALI-[BA-CH_2NH_2][BA-CH_2-NH_3^+] (red circles), MOF-808-SALI-[BA-morph]$_3$ (blue triangles) (NEM = N-ethyl morpholine. Adsorption = filled, desorption = empty markers.

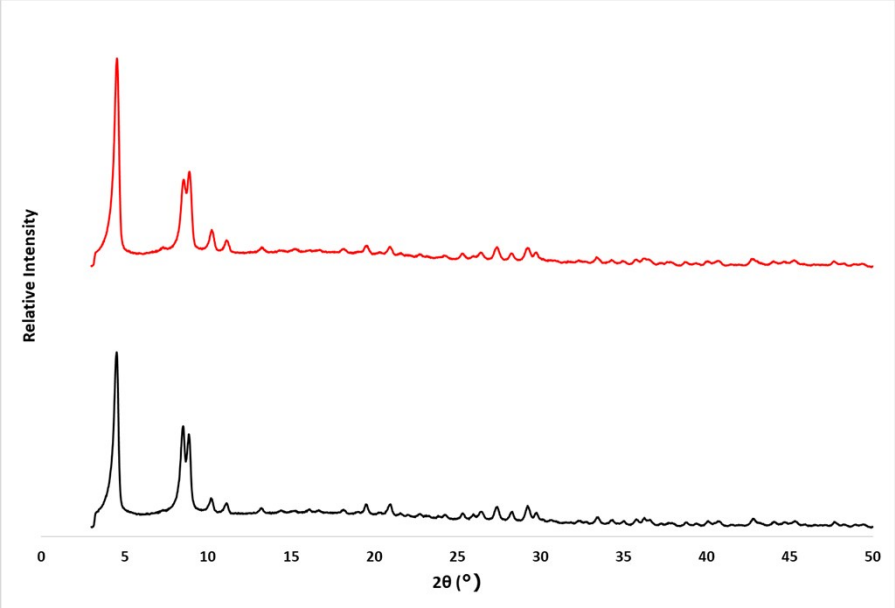

Figure S15. PXRD patterns of MOF-808-P (bottom), and DMF-HCl activated MOF-808 (top).

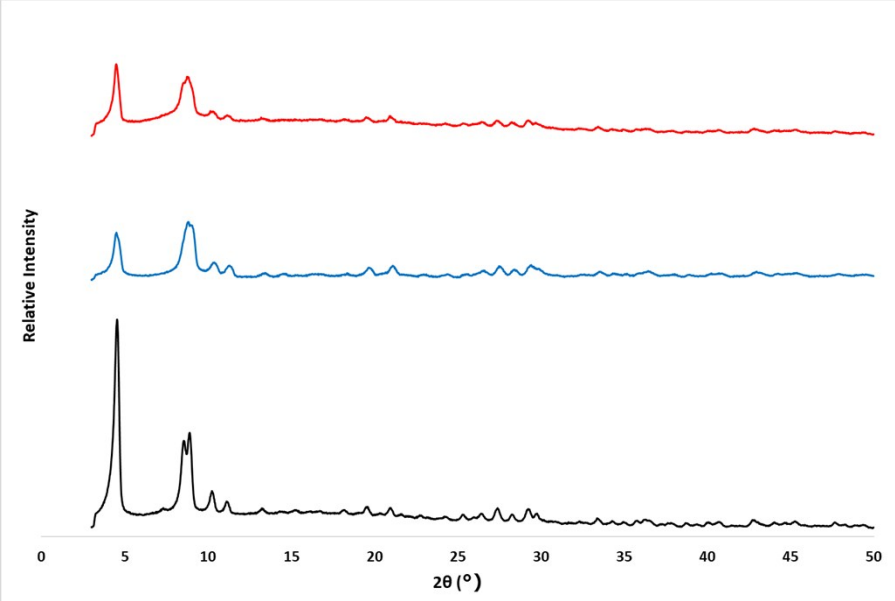

Figure S16. PXRD patterns of MOF-808-act (bottom), MOF-808-SALI-[BA-morph]$_3$ (middle), and MOF-808-SALI-[BA-CH_2NH_2][BA-CH_2-NH_3^+] (top).

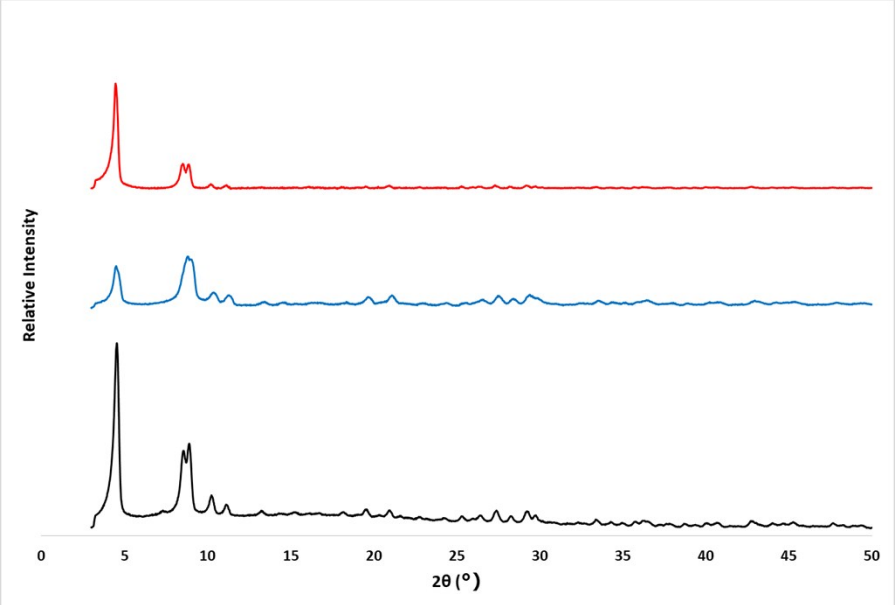

Figure S17. PXRD patterns of MOF-808-act (bottom), MOF-808-SALI-[BA-morph]$_3$ (middle), and MOF-808-SALI-[BA-morph]$_3$ post reaction (top).

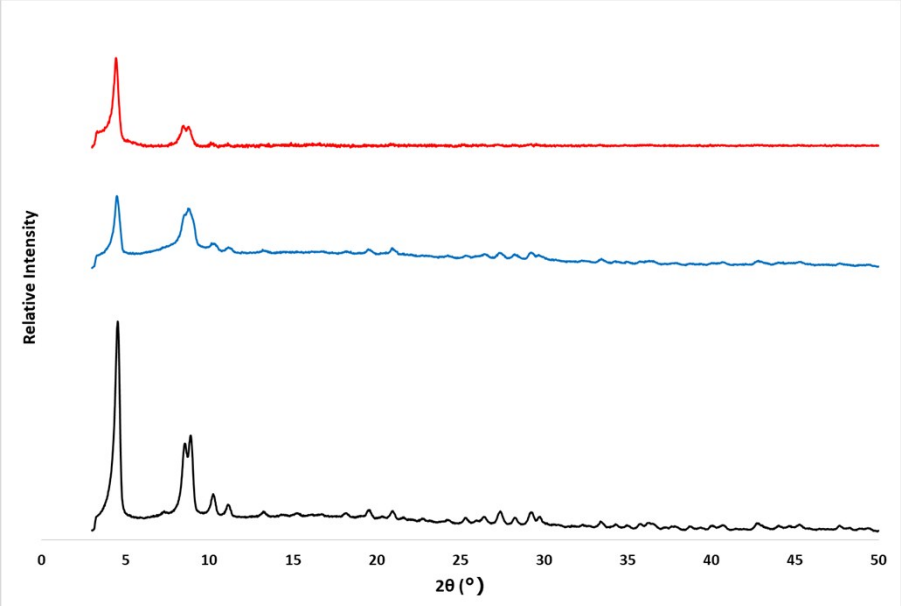

Figure S18. PXRD patterns of MOF-808-act (bottom), MOF-808-SALI-[BA-CH_2NH_2][BA-CH_2-NH_3^+] (middle), and MOF-808-SALI-[BA-CH_2NH_2][BA-CH_2-NH_3^+] post reaction (top).

DMNP hydrolysis with MOFs: MOF catalyst was added to a 1 dram vial. 1 mL of a 10% v/v D_2O/H_2O (0.1 mL D_2O, 0.9 mL DI H_2O) solution was added to the MOF. The vial was capped and sonicated briefly (~1 min) to disperse the MOF. The mixture was then transferred to an NMR tube. DMNP (25 umol, 4 uL) was added to the side of the tube via pipetter and capped. The NMR tube was quickly inverted thrice and placed into an NMR instrument. The hydrolysis was monitored by ^{31}P NMR as described above.

VX hydrolysis with MOFs: MOF catalyst was added to a 1 dram vial. 1 mL of a 10% v/v D_2O/H_2O (0.1 mL D_2O, 0.9 mL DI H_2O) solution was added to the MOF. The vial was capped and sonicated briefly (~1 min) to disperse the MOF. The mixture was then transferred to an NMR tube. DMNP (25 umol, 4 uL) was added to the side of the tube via pipetter and capped. The NMR tube was quickly inverted thrice and placed into an NMR instrument. The hydrolysis was monitored by ^{31}P NMR as described above. **Caution!!! VX is a chemical warfare agent that is highly toxic in nature, these experiments should only be performed by trained personnel using appropriate protective gear in a high-quality fume hood.**

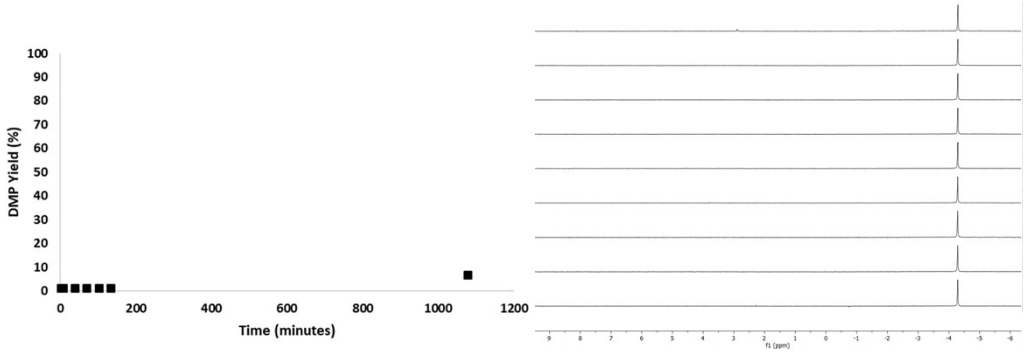

Figure S19. (Left) Plots of DMNP hydrolysis with NU-901-act at 4 mol% MOF loading. (Right) Corresponding ^{31}P NMR spectra of DMNP hydrolysis with NU-901-act at 4 mol% MOF loading.

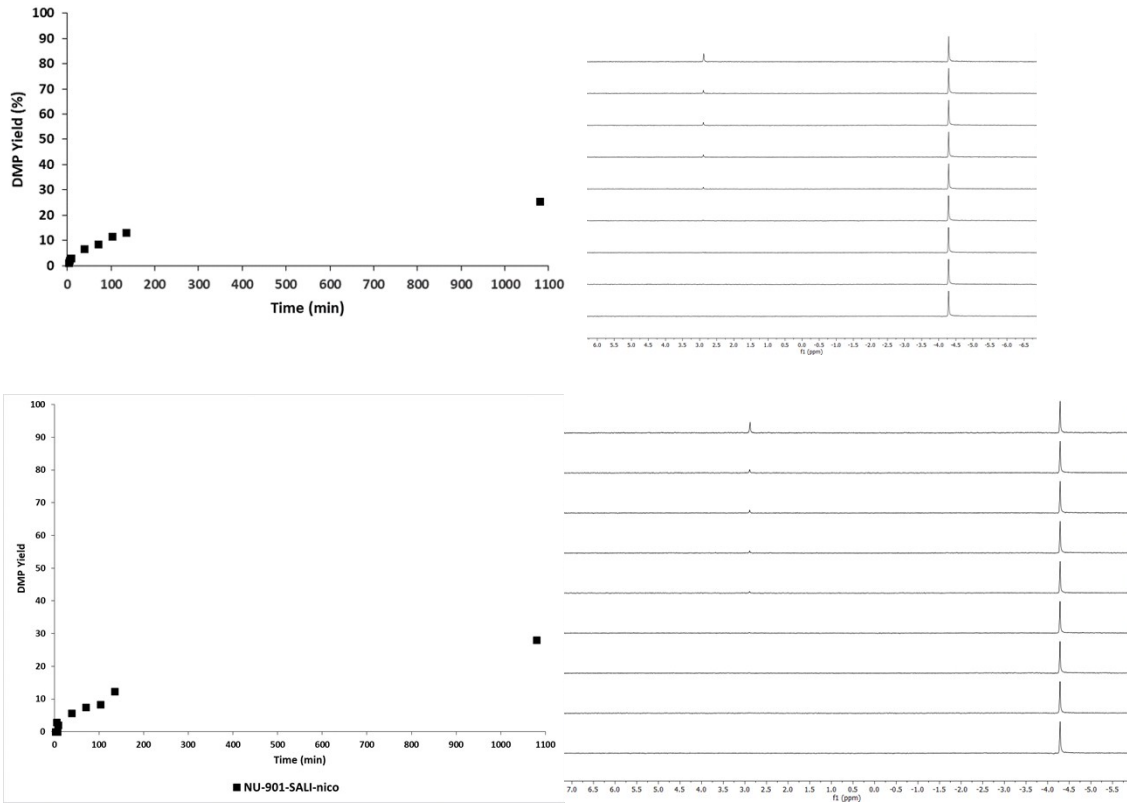

Figure S20. (Top Left) Reaction profile of DMNP hydrolysis with NU-901-SALI-[BA-N$(CH_3)_2$] at 4 mol% MOF loading. (Top Right) Corresponding ^{31}P NMR spectra of DMNP hydrolysis with NU-901-SALI-[BA-N$(CH_3)_2$]. (Bottom Left) Reaction profile of DMNP hydrolysis with NU-901-SALI-[nico]$_2$ at 4 mol% MOF loading. (Bottom Right) Corresponding ^{31}P NMR spectra of DMNP hydrolysis with NU-901-SALI-[nico]$_2$.

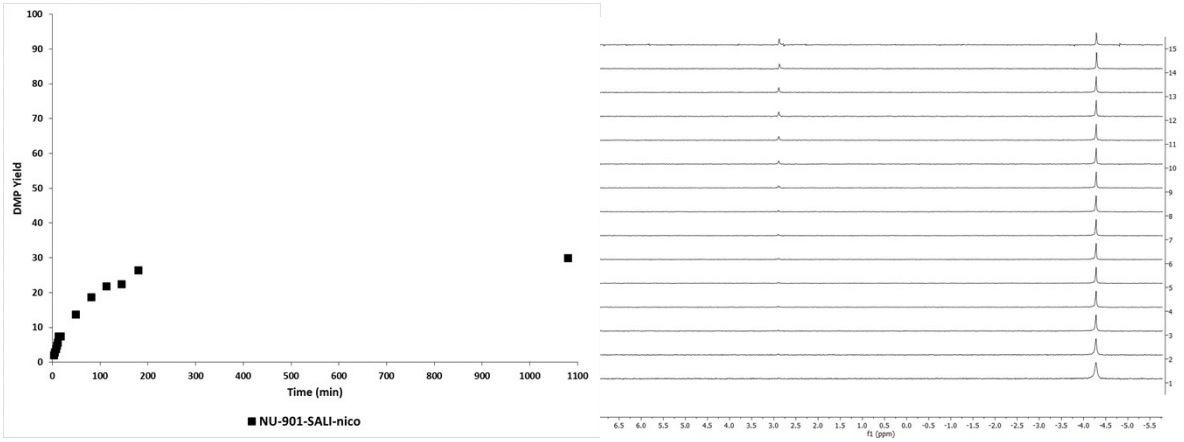

Figure S21. (Left) Reaction profile of DMNP hydrolysis with NU-901-SALI-[nico]$_2$ at 15 mol% MOF loading. (Right) Corresponding ^{31}P NMR spectra of DMNP hydrolysis with NU-901-SALI-[nico]$_2$.

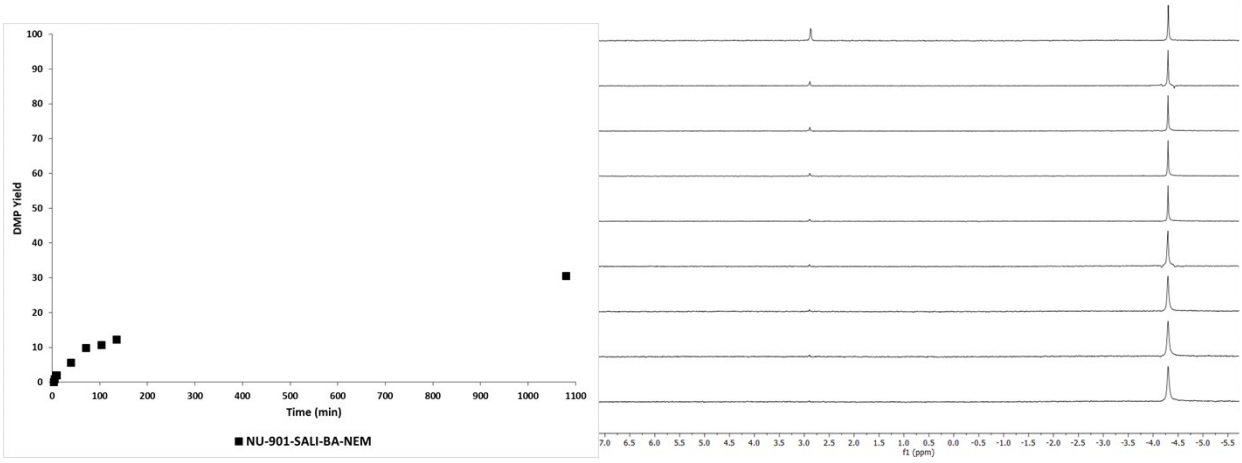

Figure S22. (Left) Reaction profile of DMNP hydrolysis with NU-901-SALI-[BA-morph]$_{3.5}$ at 9 mol% MOF loading. (Right) Corresponding ^{31}P NMR spectra of DMNP hydrolysis with NU-901-SALI-[BA-morph]$_{3.5}$.

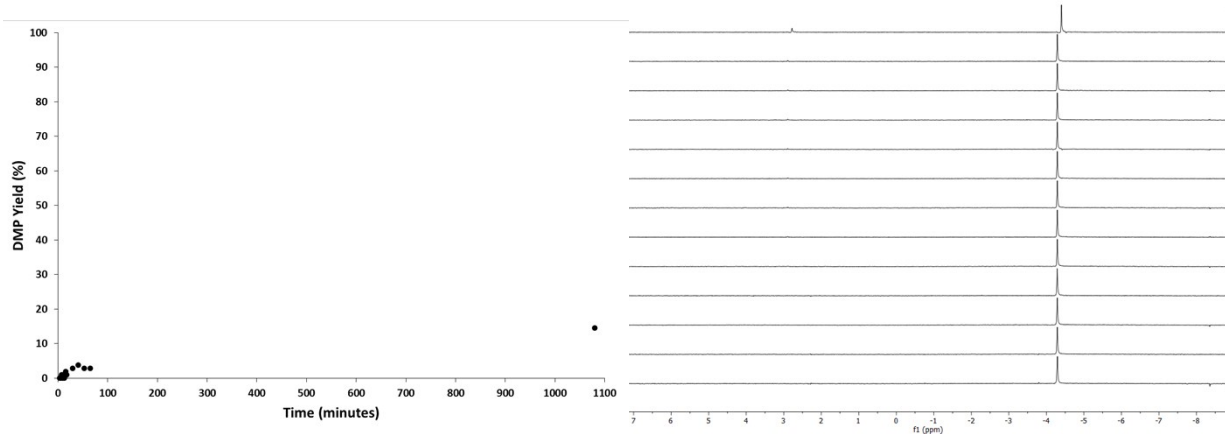

Figure S23. (Left) Reaction profile of DMNP hydrolysis with NU-901-SALI-[BA-morph]$_2$ at 9 mol% MOF loading. (Right) Corresponding ^{31}P NMR spectra of DMNP hydrolysis with NU-901-SALI-[BA-morph]$_2$.

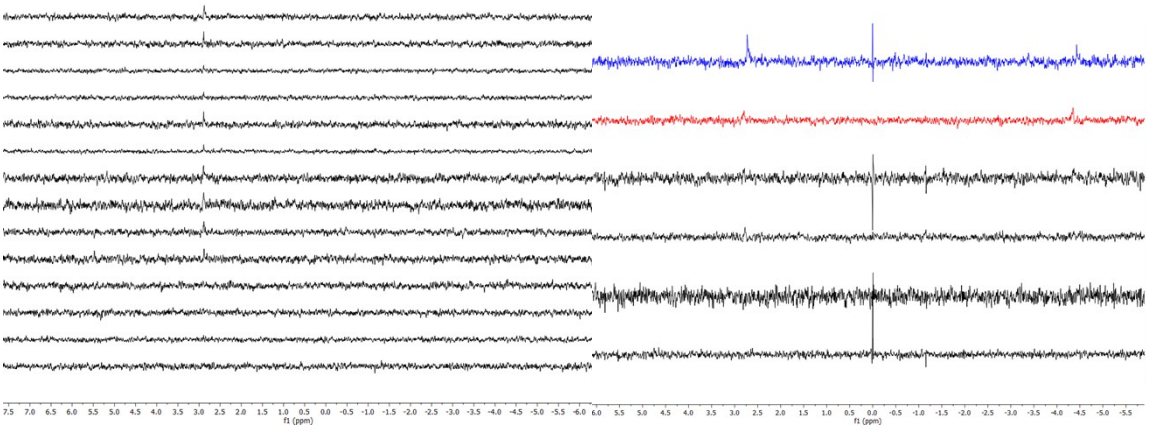

Figure S24. (Left) *in situ* ^{31}P NMR spectra of DMNP hydrolysis with NU-901-SALI-[BA-morph]$_{3.5}$ at 15 mol% MOF loading. (Right) ^{31}P NMR spectra of DMNP hydrolysis with NU-901-SALI-[BA-morph]$_{3.5}$ at 15 mol% MOF loading with filtering after 10 and 20 minutes. The bottom four spectra represent *in situ* ^{31}P NMR monitoring every two minutes (time points 2, 4, 6, 8 minutes). The red spectrum corresponds to 10 minutes while the blue corresponds to 20 minutes after filtration.

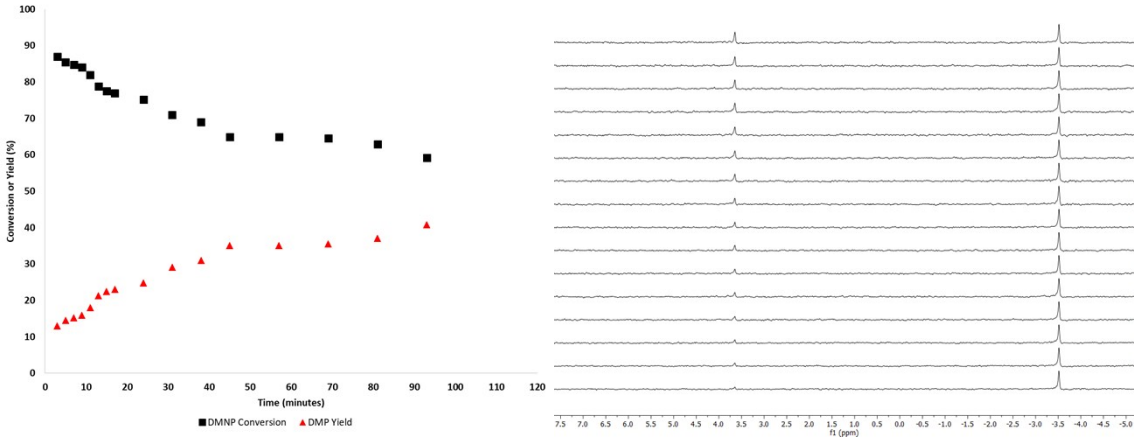

Figure S25. (Left) Reaction profile of DMNP hydrolysis with NU-901-SALI-[BA-CH_2NH_2]$_2$ at 4 mol% MOF loading. (Right) Corresponding ^{31}P NMR spectra of DMNP hydrolysis with NU-901-SALI-[BA-CH_2NH_2]$_2$.

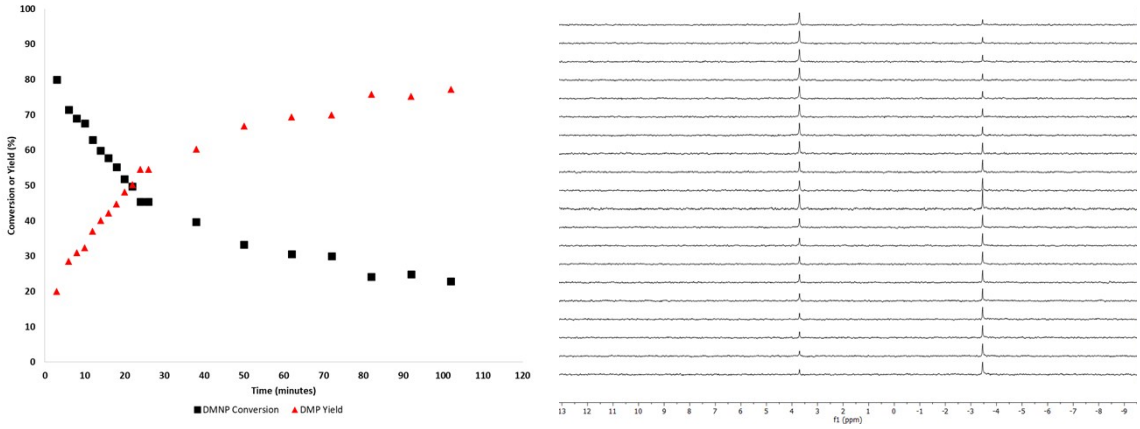

Figure S26. (Left) Reaction profile of DMNP hydrolysis with NU-901-SALI-[BA-CH_2NH_2]$_2$ at 9 mol% MOF loading. (Right) Corresponding ^{31}P NMR spectra of DMNP hydrolysis with NU-901-SALI-[BA-CH_2NH_2]$_2$.

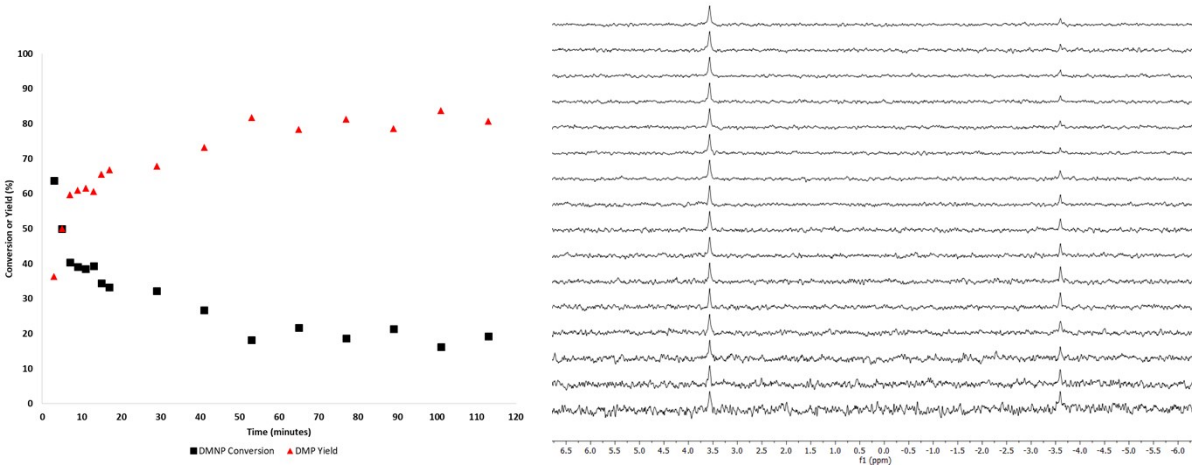

Figure S27. (Left) Reaction profile of DMNP hydrolysis with NU-901-SALI-[BA-CH_2NH_2]$_2$ at 15 mol% MOF loading. (Right) Corresponding ^{31}P NMR spectra of DMNP hydrolysis with NU-901-SALI-[BA-CH_2NH_2]$_2$.

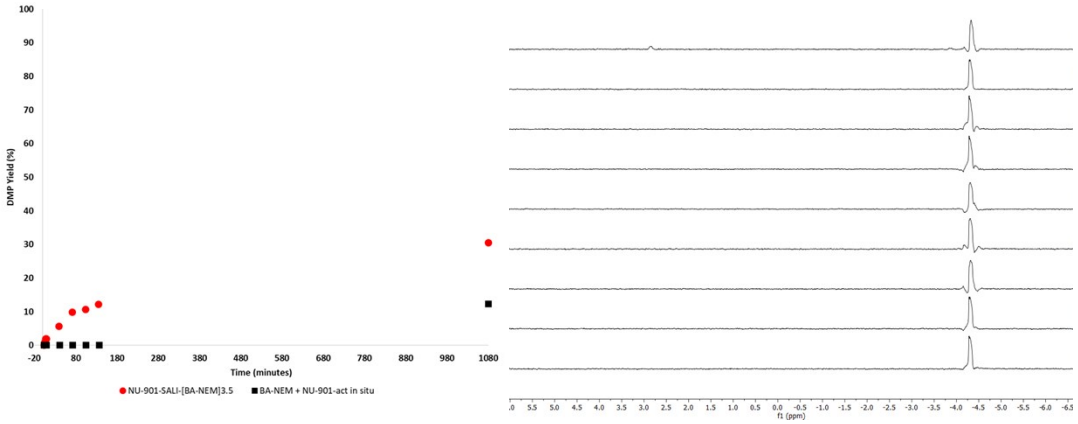

Figure S28. (Left) Plots of DMNP hydrolysis of NU-901 with *in situ* added BA-morph (black squares), and NU-901-SALI-[BA-morph]$_{3.5}$ (red circles) at 9 mol% MOF loading. (Right) Corresponding ^{31}P NMR spectra of DMNP hydrolysis with NU-901 with *in situ* added BA-morph at 9 mol% MOF loading.

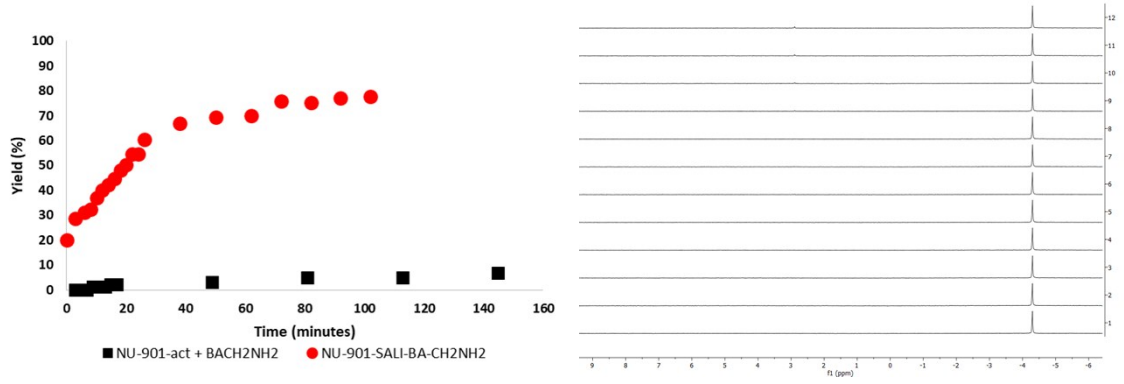

Figure S29. (Left) Plots of DMNP hydrolysis of NU-901 with *in situ* added BA-CH_2NH_2 (black squares), and NU-901-SALI-[BA-CH_2NH_2]$_2$ (red circles) at 9 mol% MOF loading. (Right) Corresponding ^{31}P NMR spectra of DMNP hydrolysis with NU-901 with *in situ* added BA-CH_2NH_2 at 9 mol% MOF loading.

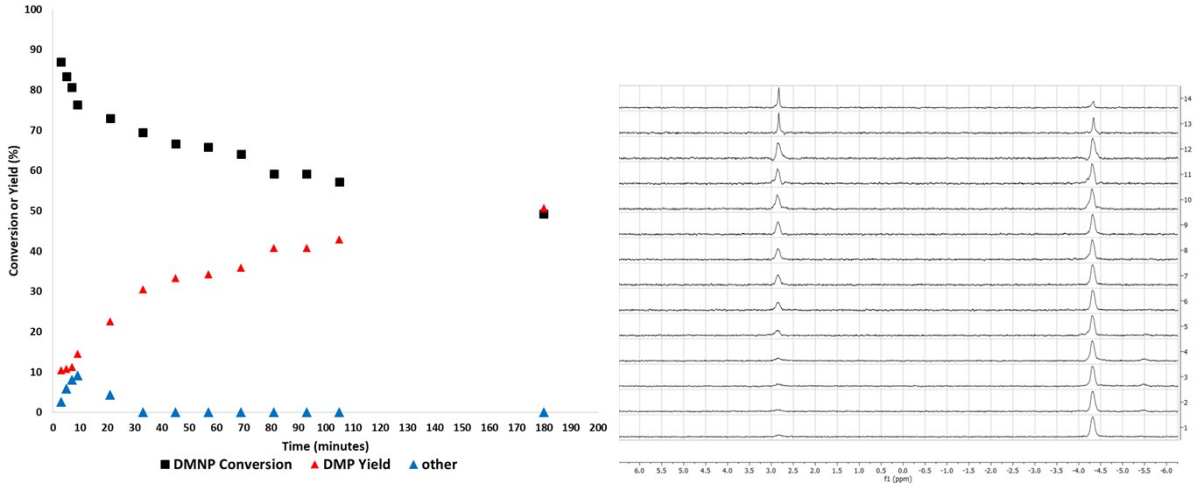

Figure S30. (Left) Reaction profile of DMNP hydrolysis with MOF-808-P at 9 mol% MOF loading. (Right) Corresponding ^{31}P NMR spectra of DMNP hydrolysis with MOF-808-P.

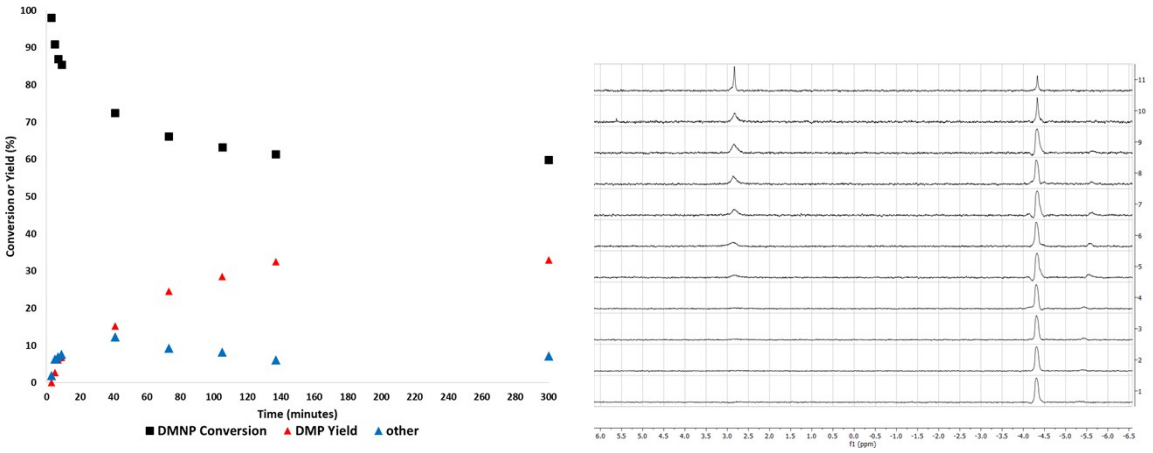

Figure S31. (Left) Reaction profile of DMNP hydrolysis with HCl-activated MOF-808 at 9 mol% MOF loading. (Right) Corresponding ^{31}P NMR spectra of DMNP hydrolysis with DMF-HCl-activated MOF-808.

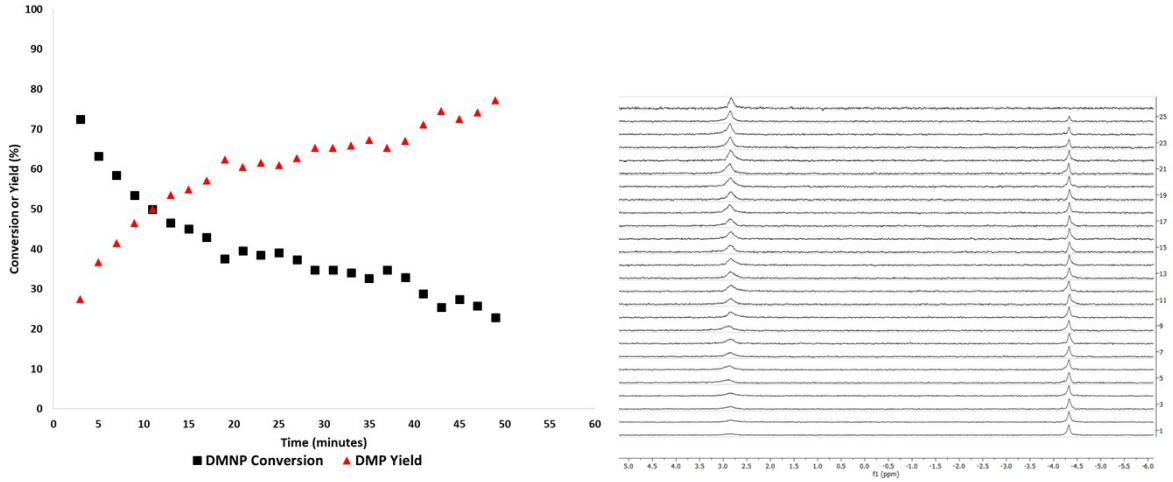

Figure S32. (Left) Reaction profile of DMNP hydrolysis with MOF-808-SALI-[BA-morph]$_3$ at 9 mol% MOF loading. (Right) Corresponding ^{31}P NMR spectra of DMNP hydrolysis with MOF-808-SALI-[BA-morph]$_3$.

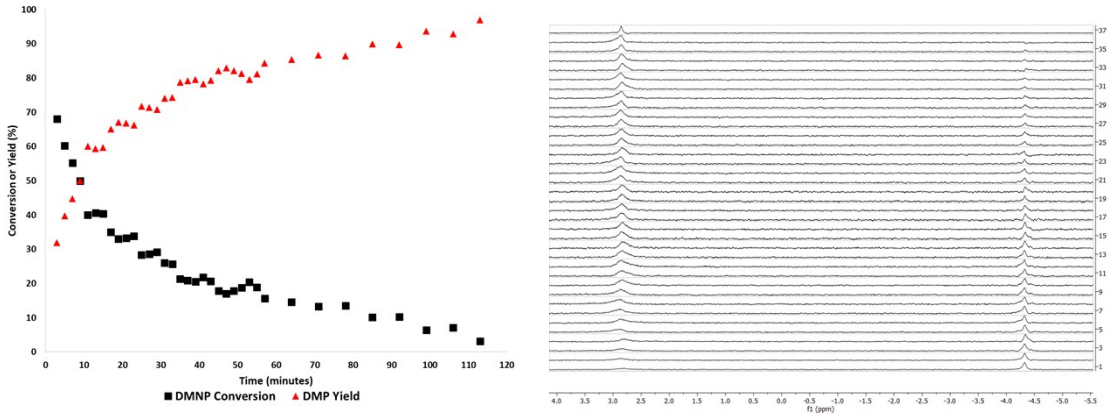

Figure S33. (Left) Reaction profile of DMNP hydrolysis with MOF-808-SALI-[BA-morph]$_3$ at 15 mol% MOF loading. (Right) Corresponding ^{31}P NMR spectra of DMNP hydrolysis with MOF-808-SALI-[BA-morph]$_3$ at 15 mol% MOF loading.

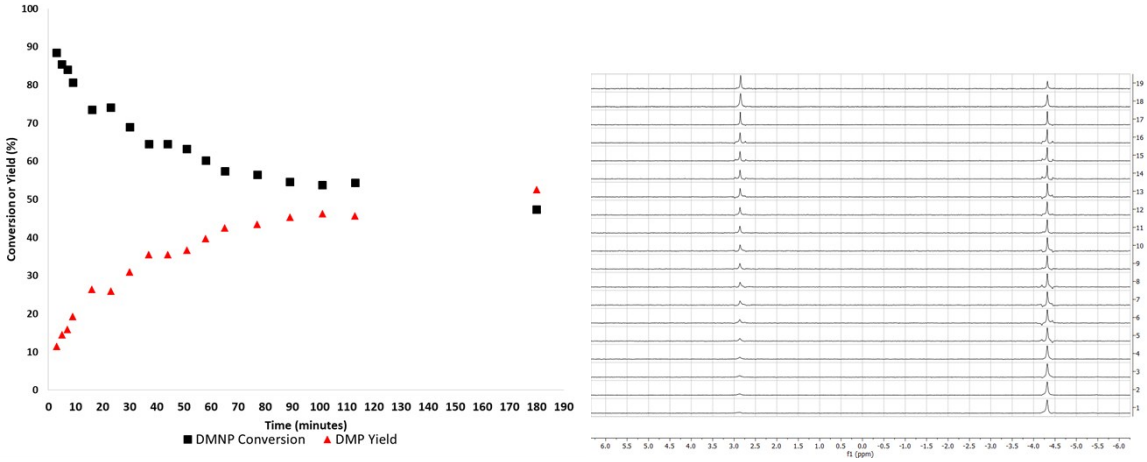

Figure S34. (Left) Reaction profile of DMNP hydrolysis with MOF-808-SALI-[BA-CH_2NH_2][BA-CH_2-$^+NH_3$] at 9 mol% MOF loading. (Right) Corresponding ^{31}P NMR spectra of DMNP hydrolysis with MOF-808-SALI-[BA-CH_2NH_2][BA-CH_2-NH_3^+] at 9 mol% MOF loading.

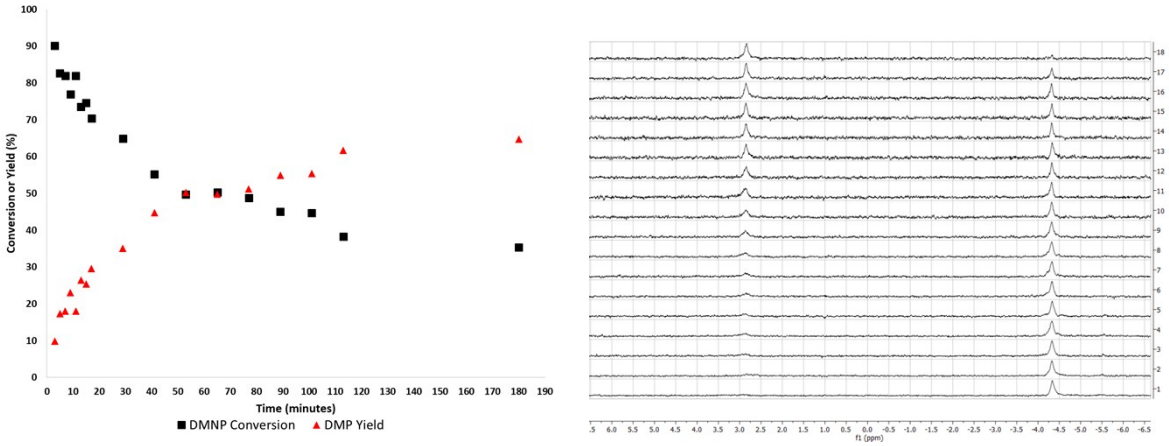

Figure S35. (Left) Reaction profile of DMNP hydrolysis with MOF-808-SALI-[BA-CH_2NH_2][BA-CH_2-NH_3^+] at 15 mol% MOF loading. (Right) Corresponding ^{31}P NMR spectra of DMNP hydrolysis MOF-808-SALI-[BA-CH_2NH_2][BA-CH_2-NH_3^+] at 15 mol% MOF loading.

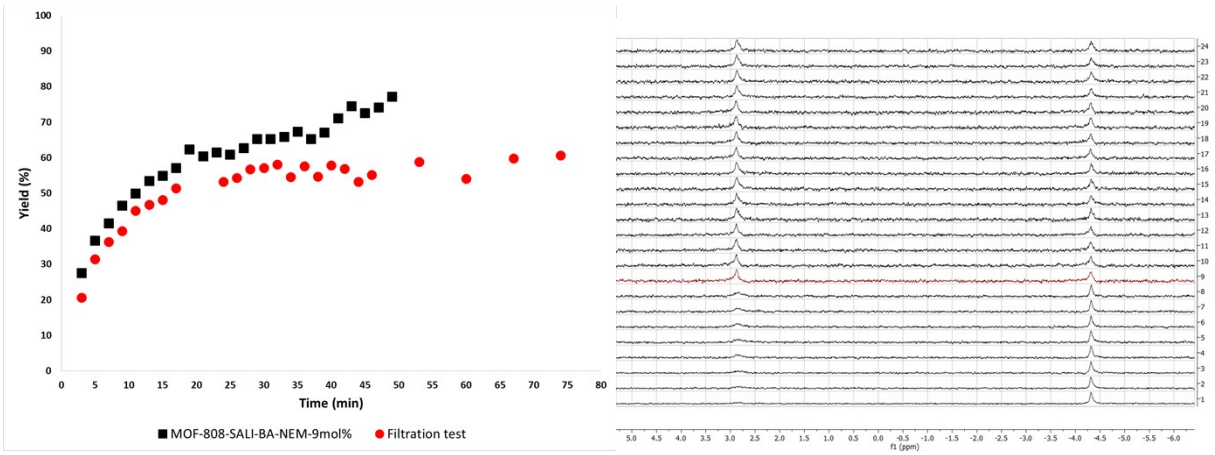

Figure S36. (Left) Reaction profile of DMNP hydrolysis with MOF-808-SALI-[BA-morph]$_3$ at 9 mol% MOF loading (black squares), and repetition with filtration at 15 min (red circles). (Right) Corresponding ^{31}P NMR spectra of DMNP hydrolysis with filtered MOF-808-SALI-[BA-morph]$_3$. The red spectrum at the 9th entry corresponds to ^{31}P NMR after filtration.

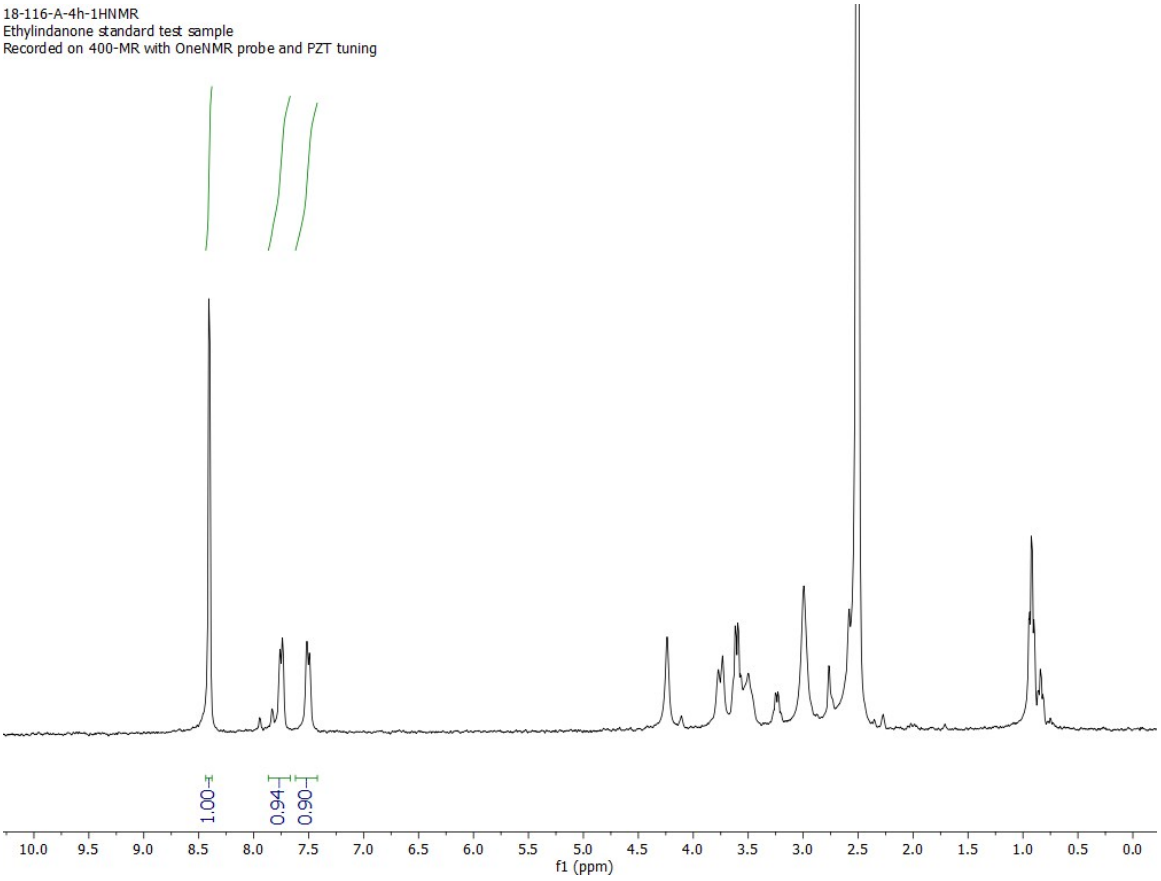

Figure S37. ^{1}H NMR spectrum of digested of MOF-808-SALI-[BA-morph]$_3$ exposed to water for 4 hours in d_6-DMSO.

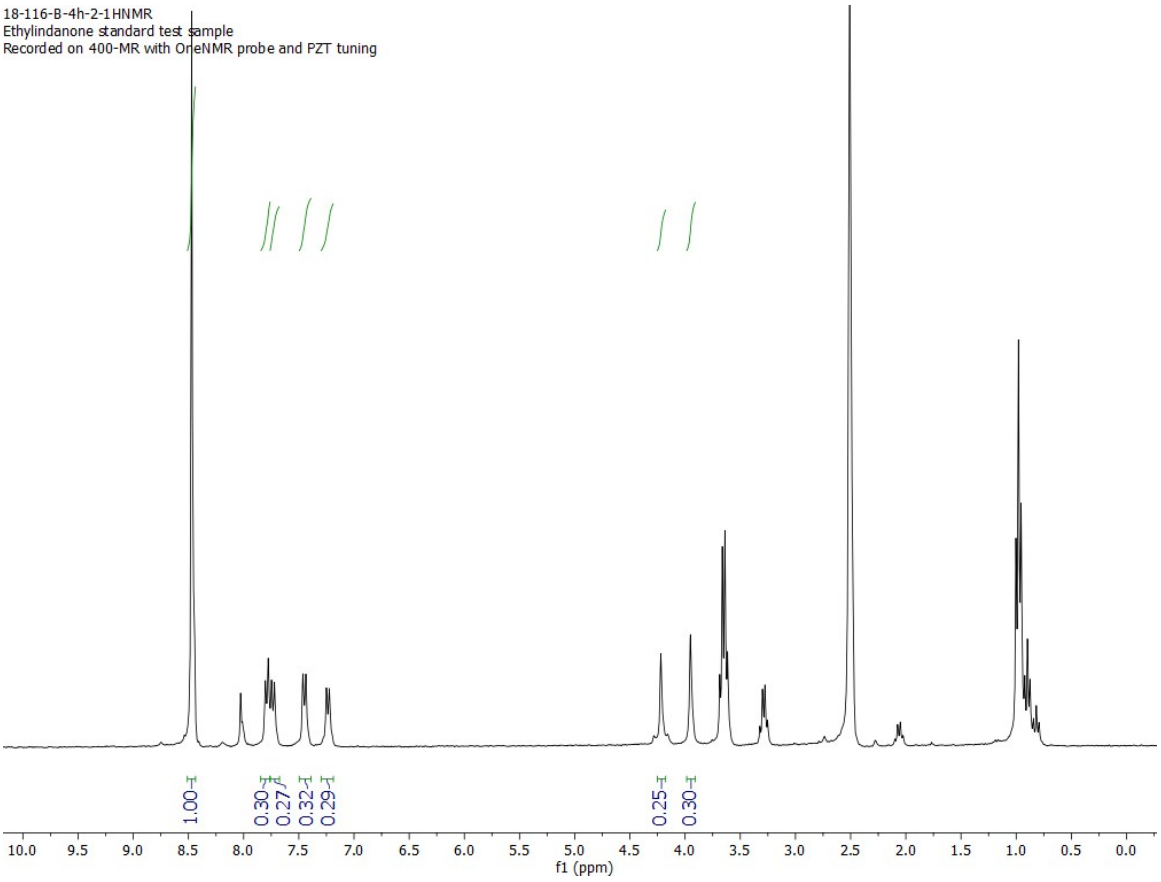

Figure S38. ^{1}H NMR spectrum of digested of MOF-808-SALI-[BA-CH_2NH_2][BA-CH_2-NH_3^+] exposed to water for 4 hours in d_6-DMSO.

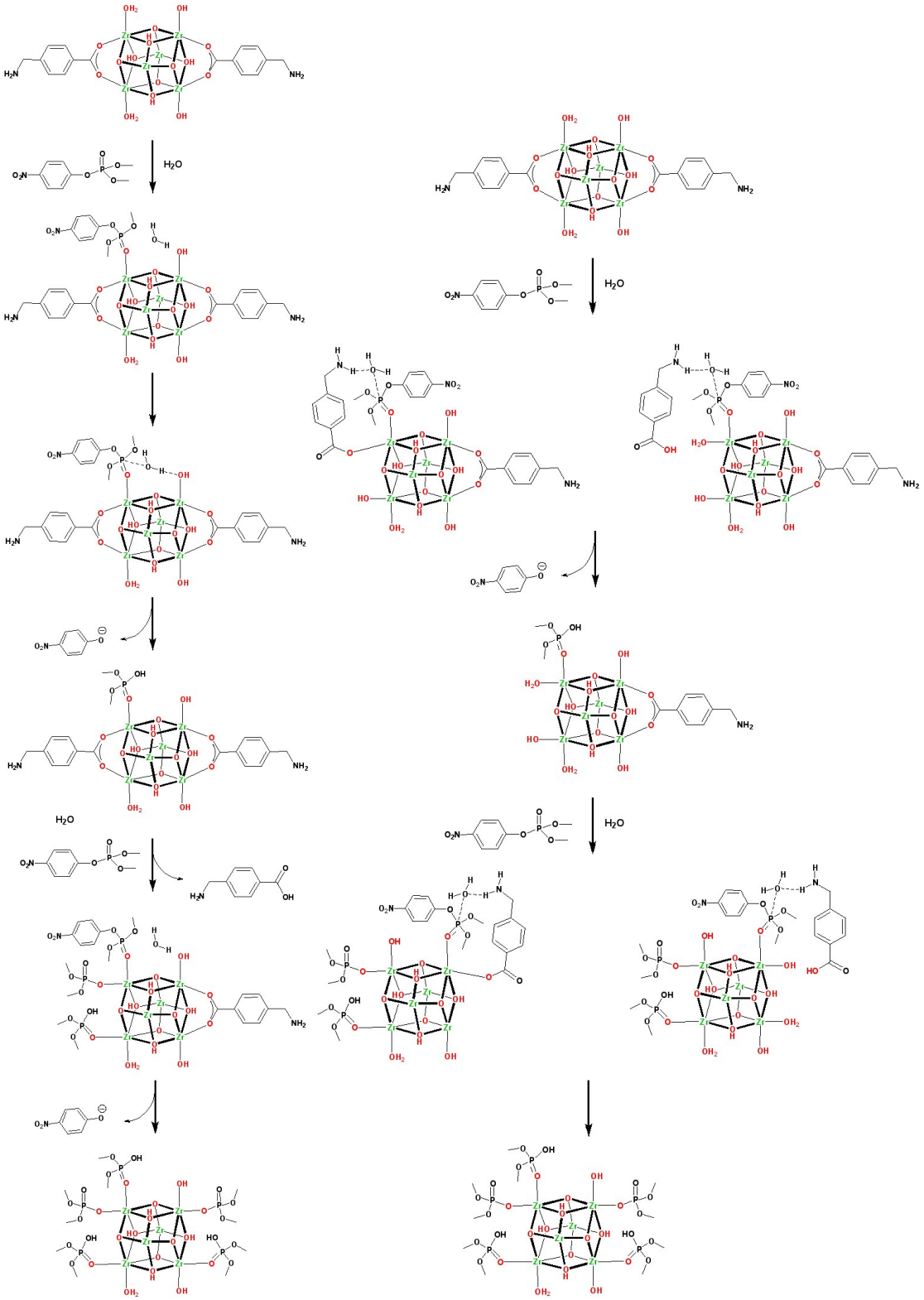

Scheme S1. Possible mechanisms of single-component MOFs. (Left) Path 1 involves hydrolysis of organophosphates with intact modulators, followed by their eventual displacement by DMP. (Right) Path 2 involves dissociated modulators participating in organophosphate hydrolysis within the sphere of the Zr_6 SBU, followed by DMP binding.

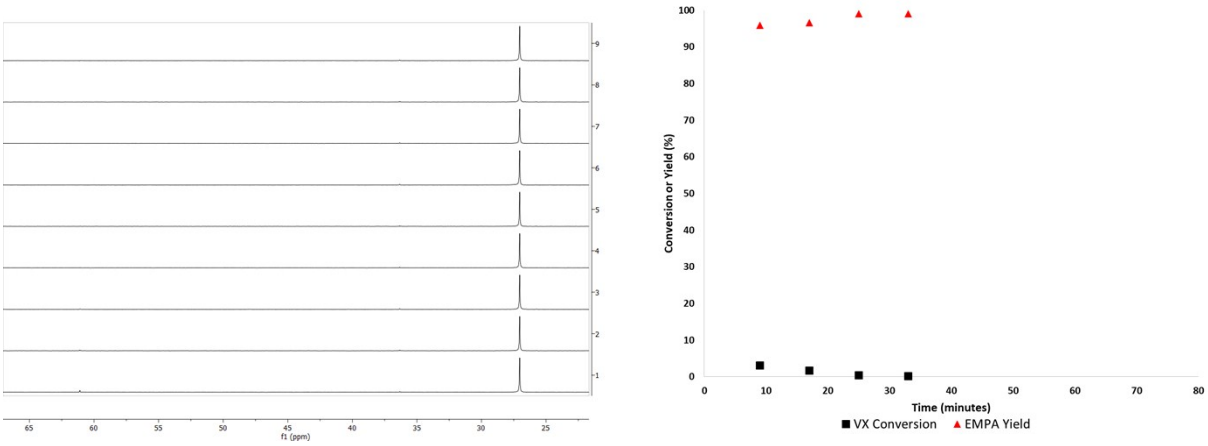

Figure S39. ^{31}P NMR spectra of VX hydrolysis with MOF-808-SALI-[BA-morph]$_3$ at 12 mol% MOF loading. VX (61 ppm), EMPA (27 ppm), and EA-2192 (36 ppm).

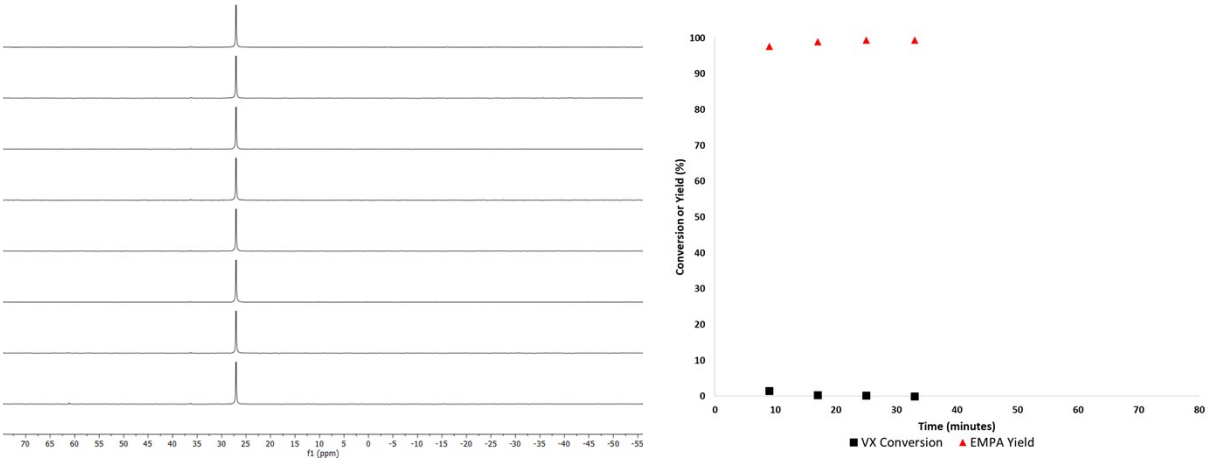

Figure S40. ^{31}P NMR spectra of VX hydrolysis with MOF-808-SALI-[BA-CH_2NH_2][BA-CH_2-NH_3^+] at 12 mol% MOF loading. VX (61 ppm), EMPA (27 ppm), and EA-2192 (36 ppm).

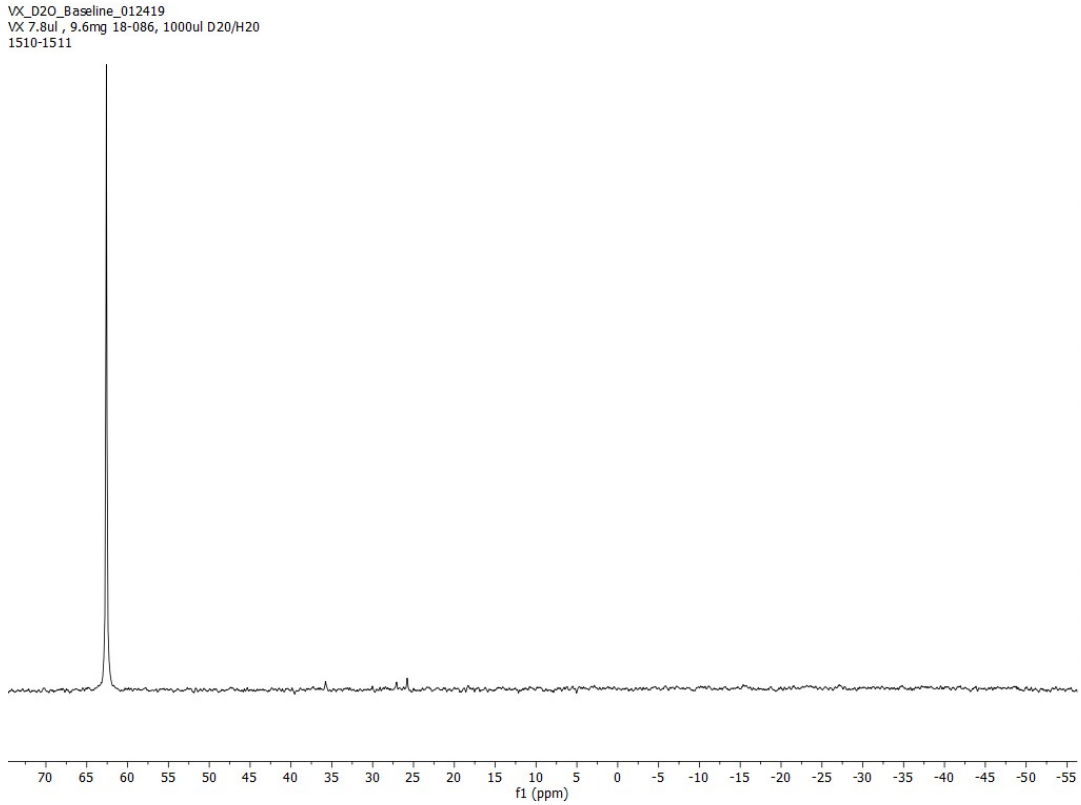

Figure S41. ^{31}P NMR spectra of VX in D_2O. VX (61 ppm), EMPA (27 ppm), and EA-2192 (36 ppm).

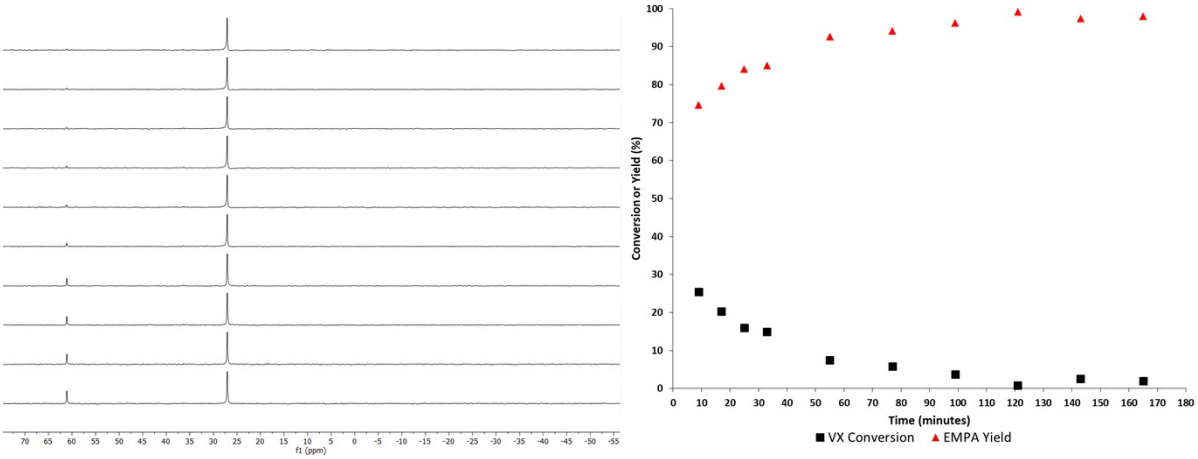

Figure S42. ^{31}P NMR spectra of VX hydrolysis with MOF-808-act at 12 mol% MOF loading. VX (61 ppm), EMPA (27 ppm), and EA-2192 (36 ppm).

Acknowledgements

We acknowledge Mr. Morgan Hall and Mr. Eric Bruni for performing VX hydrolysis experiments. O.K.F. gratefully acknowledges support from Defense Threat Reduction Agency (HDTRA1-18-1-0003) and Army Research Office-STTR (W911SR-17-C-0007). S.J.G. and J.B.D. gratefully acknowledge support by the Joint Science and Technology Office for Chemical and Biological Defense (JSTO-CBD) for support under project BA13PHM210. This research was performed while SJG held an NRC Research Associateship award at CCDC Chemical Biological Center.

References

1. J. E. Mondloch, W. Bury, D. Fairen-Jimenez, S. Kwon, E. J. DeMarco, M. H. Weston, A. A. Sarjeant, S. T. Nguyen, P. C. Stair, R. Q. Snurr, O. K. Farha and J. T. Hupp, *J. Am. Chem. Soc.*, 2013, **135**, 10294-10297.
2. T. C. Wang, N. A. Vermeulen, I. S. Kim, A. B. F. Martinson, J. F. Stoddart, J. T. Hupp and O. K. Farha, *Nature Protocols*, 2015, **11**, 149.
3. K. Inada and N. Miyaura, *Tetrahedron*, 2000, **56**, 8657-8660.
4. S. J. Garibay, I. Iordinove, T. Islamoglu, J. B. DeCoste and O. K. Farha, *CrystEngComm*, 2018, **20**, 7066-7070.